surfactant science series

volume 28

SURFACTANTS IN CHEMICAL / PROCESS ENGINEERING

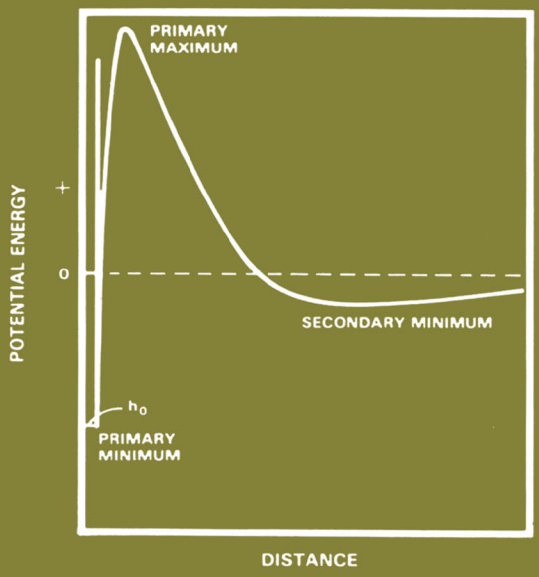

edited by

Darsh T. Wasan
Martin E. Ginn
Dinesh O. Shah

SURFACTANTS IN CHEMICAL/ PROCESS ENGINEERING

SURFACTANT SCIENCE SERIES

CONSULTING EDITORS

MARTIN J. SCHICK
Consultant
New York, New York

FREDERICK M. FOWKES
Department of Chemistry
Lehigh University
Bethlehem, Pennsylvania

Volume 1: NONIONIC SURFACTANTS, edited by Martin J. Schick

Volume 2: SOLVENT PROPERTIES OF SURFACTANT SOLUTIONS, edited by Kozo Shinoda (*out of print*)

Volume 3: SURFACTANT BIODEGRADATION, by R. D. Swisher *(See Volume 18)*

Volume 4: CATIONIC SURFACTANTS, edited by Eric Jungermann

Volume 5: DETERGENCY: THEORY AND TEST METHODS (*in three parts*), edited by W. G. Cutler and R. C. Davis

Volume 6: EMULSIONS AND EMULSION TECHNOLOGY (*in three parts*), edited by Kenneth J. Lissant

Volume 7: ANIONIC SURFACTANTS (*in two parts*), edited by Warner M. Linfield

Volume 8: ANIONIC SURFACTANTS–CHEMICAL ANALYSIS, edited by John Cross

Volume 9: STABILIZATION OF COLLOIDAL DISPERSIONS BY POLYMER ADSORPTION, by Tatsuo Sato and Richard Ruch

Volume 10: ANIONIC SURFACTANTS–BIOCHEMISTRY, TOXICOLOGY, DERMATOLOGY, edited by Christian Gloxhuber

Volume 11: ANIONIC SURFACTANTS–PHYSICAL CHEMISTRY OF SURFACTANT ACTION, edited by E. H. Lucassen-Reynders

Volume 12: AMPHOTERIC SURFACTANTS, edited by B. R. Bluestein and Clifford L. Hilton

Volume 13: DEMULSIFICATION: INDUSTRIAL APPLICATIONS, by Kenneth J. Lissant

Volume 14: SURFACTANTS IN TEXTILE PROCESSING, by Arved Datyner

Volume 15: ELECTRICAL PHENOMENA AT INTERFACES: FUNDAMENTALS, MEASUREMENTS, AND APPLICATIONS, edited by Ayao Kitahara and Akira Watanabe

Volume 16: SURFACTANTS IN COSMETICS, edited by Martin M. Rieger

Volume 17: INTERFACIAL PHENOMENA: EQUILIBRIUM AND DYNAMIC EFFECTS, by Clarence A. Miller and P. Neogi

Volume 18: SURFACTANT BIODEGRADATION, Second Edition, Revised and Expanded, by R. D. Swisher

Volume 19: NONIONIC SURFACTANTS: CHEMICAL ANALYSIS, edited by John Cross

Volume 20: DETERGENCY: THEORY AND TECHNOLOGY, edited by W. Gale Cutler and Erik Kissa

Volume 21: INTERFACIAL PHENOMENA IN APOLAR MEDIA, edited by Hans-Friedrich Eicke and Geoffrey D. Parfitt

Volume 22: SURFACTANT SOLUTIONS: NEW METHODS OF INVESTIGATION, edited by Raoul Zana

Volume 23: NONIONIC SURFACTANTS: PHYSICAL CHEMISTRY, edited by Martin J. Schick

Volume 24: MICROEMULSION SYSTEMS, edited by Henri L. Rosano and Marc Clausse

Volume 25: BIOSURFACTANTS AND BIOTECHNOLOGY, edited by Naim Kosaric, W. L. Cairns, and Neil C. C. Gray

Volume 26: SURFACTANTS IN EMERGING TECHNOLOGIES, edited by Milton J. Rosen

Volume 27: REAGENTS IN MINERAL TECHNOLOGY, edited by P. Somasundaran and Brij M. Moudgil

Volume 28: SURFACTANTS IN CHEMICAL/PROCESS ENGINEERING, edited by Darsh T. Wasan, Martin E. Ginn, and Dinesh O. Shah

Volume 29: THIN LIQUID FILMS, edited by I. B. Ivanov

Volume 30: MICROEMULSIONS AND RELATED SYSTEMS: FORMULATION, SOLVENCY, AND PHYSICAL PROPERTIES, edited by Robert S. Schecter and Maurice Bourrel

Volume 31: CRYSTALLIZATION AND POLYMORPHISM OF FATS AND FATTY ACIDS, edited by Nissim Garti and K. Sato

Volume 32: INTERFACIAL PHENOMENA IN COAL TECHNOLOGY, edited by Gregory D. Botsaris and Yuli M. Glazman

SURFACTANTS IN CHEMICAL/ PROCESS ENGINEERING

edited by

Darsh T. Wasan
Department of Chemical Engineering
Illinois Institute of Technology
Chicago, Illinois

Martin E. Ginn
Stuart School of Business Administration
Illinois Institute of Technology
Chicago, Illinois

Dinesh O. Shah
Department of Chemical Engineering and
Center for Surface Science and Engineering
University of Florida
Gainesville, Florida

Marcel Dekker, Inc. **New York and Basel**

Library of Congress Cataloging in Publication Data

Surfactants in chemical.

(Surfactant science series ; v. 28)
Includes index.
1. Surface active agents. I. Wasan, Darsh T.
II. Ginn, Martin E. III. Shah, Dinesh O.
(Dinesh Ochhavlal) IV. Series.
TP994.S874 1988 668'.1 88-3869
ISBN 0-8247-7830-8

MARCEL DEKKER, INC.
270 Madison Avenue, New York, New York 10016

Current printing (last digit):
10 9 8 7 6 5 4 3 2 1

PRINTED IN THE UNITED STATES OF AMERICA

Preface

Surfactants are an interesting class of materials, and it is their dual characteristics (hydrophilic-lipophilic nature) that make them so useful. Surfactants play an important role in many processes ranging from the very mundane (washing cloth) to the very sophisticated (microelectronics). In the last several years, there has been a great deal of research activity in understanding the role of surfactants in multi-billion-dollar chemical and processing industries. Rates of organic reactions have been shown to be accelerated by many orders of magnitude by carrying out the reactions in appropriate micellar or microemulsion media. New examples include the application of surfactants in unit operations for industrial separations, environmental protection, pharmaceuticals, herbicides and pesticides, engineered materials, and enhanced oil recovery. (The reader is referred to Volume 26 of this series, *Surfactants in Emerging Technologies*, edited by Milton J. Rosen.) All these new developments in the field of surfactants obviously cannot be covered in one volume. However, we have made an attempt to focus on a few of the recent developments in industrial applications of surfactants and to bridge the gap from engineering science to application technology.

In recent years, there has been more involvement by chemical engineers and applied chemists in the process application of surfactants and hence greater willingness on their part to address this important subject. Therefore, it should not be very surprising that most of the contributors to this volume are engineering scientists.

The various chapters may be outlined as follows. The field of surface rheology has largely developed over the past two decades. Edwards and Wasan, in the first chapter, introduce the reader to

surface rheological properties such as surface shear and dilatational viscosities and elasticities of fluid-fluid interfaces containing surfactants by using a simplified "pillbox" approach. They then proceed to show the importance of these properties in practical dynamic surface problems with particular emphasis on the role that the dilatational surface properties play in a number of applications involving the use of surfactants such as foam rheology, foam flow in enhanced oil recovery, and foam and emulsion stability.

Distillation is a complex vapor-liquid contacting operation, but it lies at the heart of many process industries. Berg describes the observed effects of surfactants in distillation processes. Surface-tension effects, and their modification by surface-active agents, play a significant role in the performance of distillation equipment. Traces of surfactants have been shown to be capable of improving the performance of packed distillation towers by as much as 80%. Enhancement is achieved through the stabilization against rupture of the thin films of reflux liquid flowing over the irrigated packing, thereby increasing available interfacial area. Similar area increases can be achieved for tray columns through the stabilization of froths. These effects are described, explained, and quantified by both hydrodynamic analyses and laboratory experiments using bench-scale equipment.

Scamehorn and Harwell provide an in-depth examination of how surfactant systems can be used in the treatment of aqueous process streams to achieve important industrial separations. Five important separation techniques are examined, namely, micellar-enhanced ultrafiltration, foam separations, surfactant-enhanced carbon regeneration, extraction into reverse micelles, and admicellar chromatography. These methods are of special interest because they typically require low energy for operation. They are also quite useful in selectively removing organics or multivalent ions from water, in addition to other separations. Accordingly, surfactant-based separations are useful for separating contaminants or for enrichment of value components. Technologies in which these techniques may be widely used include biotechnology applications, pollution control or waste water treatment, and separation of metals.

Li invented the liquid surfactant membrane concept in 1968. Over the last 20 years, considerable efforts by chemists and chemical engineers have been devoted to developing the liquid surfactant membranes for many potential applications, including separation of hydrocarbons, hydrometallurgy, waste water treatment, biomedicine, and biochemical engineering. To date, this concept has been successfully commercialized for the extraction of metals. Gu, Wasan, and Li specifically review the various extraction systems for metal ion recovery and the dominant mechanisms for their extraction.

Sonntag examines the use of surfactants in the aqueous separation of two important fatty acids, oleic and stearic acids, from

mixtures of tallow fatty acids. He includes a discussion of some fundamental properties such as adsorption, wetting, and hydrophilization in treating his topic. Aqueous emulsion separations are shown to offer advantages over solidification and solvent crystallization methods based on melting-point differences. Adsorption and wetting are shown to be especially important in separating oleic from stearic acid. Successful separations are achieved by treating the fatty acid mixtures with solutions of 0.5% (by weight) sodium lauryl sulfate and 2% (by weight) magnesium sulfate, followed by centrifuging or rotary vacuum filtration. Surfactant concentrations are regarded as critical since highly emulsified mixtures are found to separate only with great difficulty. The results are discussed in relation to key surface and wetting phenomena.

Somasundaran and Ramachandran review the role of surfactants in flotation, an important unit operation. The principles that govern surfactant adsorption and particle-bubble attachment are discussed with relevant examples from the literature. Selective adsorption of surfactants on particles is dependent on the surface and solubility properties of the solid and the solution chemistry of the surfactants, as well as on the dissolved inorganics and polymers present in the system. The importance of the interactions of the different species of the surfactants with inorganics, as well as with polymers in bulk and at various interfaces, is emphasized. Effects of the different variables such as pH, ionic strength, and temperature are also discussed.

A second chapter by Sonntag deals with the role of surfactants in herbicide emulsions. Surfactants are shown to play a vital role in weed control technology by increasing the effectiveness of herbicides. The action of surfactants relates to their ability to accomplish a more uniform distribution over the surface of leaf foliage (and also by increasing penetration). Factors affecting surfactant usefulness in herbicide dispersion include surface activity (surface-tension lowering), wetting properties, contact angle, micelle formation, and hydrophobic-lipophilic balance (HLB), particularly for nonionic surfactants. The increased use of vegetable oils in herbicide dispersions as replacements for hydrocarbons (and water) is discussed in developing an understanding of these complex systems. Factors favoring use of vegetable oils such as soybean oil include ready availability, improved functionality, and better environmental acceptance. Such factors tend to override costs in many situations.

Kine and Redlich provide a thorough treatment of the role of surfactants in emulsion polymerization. The product of such polymerization is termed "emulsion polymer," a latex or a polymeric dispersion, and consists of minute plastic spheres (10^{-4} mm in diameter) dispersed in a continuous phase, usually water. Each cubic centimeter of latex contains about 100 trillion of these spheres, and

each sphere has a layer of a surface-active moiety on its surface. The use of surfactants is shown to be vital in the preparation of the emulsion polymer and, at times, of even greater importance in its formulation and application (e.g., in protective coatings). Factors affecting the preparation of the dispersion, the resulting physical properties, and ultimate application are discussed in developing a greater understanding of interrelationships. Whenever possible, the authors strive to develop both theoretical and practical implications pertinent to various industrial applications. Such applications of emulsion polymers include use in soil stabilizers, protective coatings, sealants, adhesives, tile and paper finishing agents, and specialty concretes, and for the treatment of automotive and aircraft tires.

The late Dr. J. Schulman, mentor of Shah, coined the word "microemulsion." A microemulsion can be defined as a thermodynamically stable, isotopically clear dispersion of two immiscible liquids, consisting of microdomains of one or both liquids stabilized by an interfacial film of surface-active molecules. Since the introduction of microemulsions in 1943, significant advances have been made to explain the formation, structure, properties, and phase behavior of microemulsions. Leung, Hou, and Shah review the various theoretical and experimental aspects, as well as novel applications of microemulsions.

The last chapter, by Woods and Diamadopoulos, reviews the fundamentals of surface phenomena that affect stability of dispersions. Included are equilibrium theories of electrochemical double layer and adsorbed macromolecule and rate theories of coalescence, adsorption, and coagulation. Eleven strategies that affect stability are outlined. The role of surfactants, inorganics and polymers, and solubility are discussed. Methods are given to predict the drop size and to characterize dispersions. Overall strategies and rules of thumb for separation dispersions are presented. Details are given for chemical destabilization, coagulation and flocculation, and deep-bed filtration and flotation. Numerous practical sample calculations are given.

We wish to thank all the authors for their contributions and for providing us with the summaries of their work that are included in this preface. We have attempted to cover some recently selected developments to highlight the importance of surfactants and surface phenomena, and the use of surfactants and the role they play in various applications. We hope this volume, although far from being comprehensive, will be judged as definitive and will stimulate other works to further enhance our knowledge in this technologically important field.

Darsh T. Wasan

Martin E. Ginn

Dinesh O. Shah

Contributors

John C. Berg Department of Chemical Engineering, University of Washington, Seattle, Washington

Evan Diamadopoulos Department of Chemical Engineering, McMaster University, Hamilton, Ontario, Canada

D. A. Edwards Department of Chemical Engineering, Illinois Institute of Technology, Chicago, Illinois

*Z. M. Gu** Department of Chemical Engineering, Illinois Institute of Technology, Chicago, Illinois

Jeffrey H. Harwell Institute for Applied Surfactant Research, University of Oklahoma, Norman, Oklahoma

Mean Jeng Hou Department of Chemical Engineering and Center for Surface Science and Engineering, University of Florida, Gainesville, Florida

Benjamin B. Kine Research Labs, Rohm and Haas Company, Spring House, Pennsylvania

Roger Leung † Department of Chemical Engineering and Center for Surface Science and Engineering, University of Florida, Gainesville, Florida

Present affiliation:
*Institute of Atomic Energy, Academia Sinica, Beijing, China.
†Aluminum Company of America, Alcoa Center, Pennsylvania.

Norman N. Li Allied-Signal, Inc., Des Plaines, Illinois

R. Ramachandran Henry Krumb School of Mines, Columbia University, New York, New York

George H. Redlich Research Labs, Rohm and Haas Company, Spring House, Pennsylvania

John F. Scamehorn Institute for Applied Surfactant Research, University of Oklahoma, Norman, Oklahoma

Dinesh O. Shah Department of Chemical Engineering and Center for Surface Science and Engineering, University of Florida, Gainesville, Florida

P. Somasundaran Henry Krumb School of Mines, Columbia University, New York, New York

Norman O. V. Sonntag Consultant, Red Oak, Texas

Darsh T. Wasan Department of Chemical Engineering, Illinois Institute of Technology, Chicago, Illinois

Donald R. Woods Department of Chemical Engineering, McMaster University, Hamilton, Ontario, Canada

Contents

SURFACTANTS IN CHEMICAL/ PROCESS ENGINEERING

1

Dilatational Properties of Adsorbed Surfactant Interfaces and Their Applications

D. A. EDWARDS and DARSH T. WASAN *Illinois Institute of Technology, Chicago, Illinois*

I. INTRODUCTION

The adsorption of surfactant at a fluid-fluid interface has long been known to alter equilibrium interfacial properties. However, in practice, equilibrium is an inevitable abstraction: the limiting case of actual dynamic processes which occur near, at, and across an interface. Dynamic interfacial properties, which are required to quantify practical dynamic surface problems, are less well known.

Dynamic interfacial properties may be classified in terms of shear properties and dilatational properties. The former, which typically include the surface shear viscosity and the shear elasticity, have

been shown relevant to such dynamic phenomena as foam and emulsion stability, coalescence, and interfacial mass transfer [1–3].

We have recently undertaken a fundamental research program to investigate the less understood but more significant dilatational properties, such as the dynamic surface/interfacial tension, the dilatational modulus, and the surface dilatational viscosity. Our objective in this research has been first, to develop techniques to measure the dilatational properties, and second, to investigate (both experimentally and theoretically) the correlation between the dynamic surface/interfacial properties and foam rheology, foam flow in EOR processes, foam stability, and emulsion stability.

In this chapter we summarize the current results from our research efforts, beginning with a simple derivation of the relation between surface and bulk-phase hydrodynamics (in which context dynamic surface properties are defined), followed by a detailed consideration of surface dilatational properties, and concluding with the various theoretical and experimental results that we have obtained for dilatational surface properties and their application to dynamic interfacial phenomena.

II. DYNAMIC SURFACE PROPERTIES (SURFACE RHEOLOGY)

Surface rheology is the study of interfacial response to deformation. Often we consider the deformational response of the surface as defined by a single stress coefficient: the surface tension. However, when surfactant adsorbs to the fluid-fluid interface, an intrinsic rigidity may arise, introducing beyond the tensile response to deformation, a damping or viscous response which cannot be defined completely by the surface tension, requiring coefficients of surface viscosity.

Although the origin of surface tension and surface viscosities is quite intuitive, the surface stress equations that relate these stress coefficients to the deformational response of the surface soon lose intuitive appeal, particularly when the surface becomes curved. Therefore, to advance an intuitive understanding of surface rheology we will throughout this section consider the rheology of the planar fluid surface. The reader interested in the rheology of curved fluid surfaces is referred to Refs. 4 and 5.

Consider, then, a rectangular fluid element containing a portion of two continuous fluid phases, as in Fig. 1. The thickness of the element (2ℓ) is sufficiently small that the inhomogeneous layer of fluid between the two fluid phases loses any discontinuous appearance. This inhomogeneous layer, the interfacial region, is completely contained between the surfaces $z = \pm\ell$.

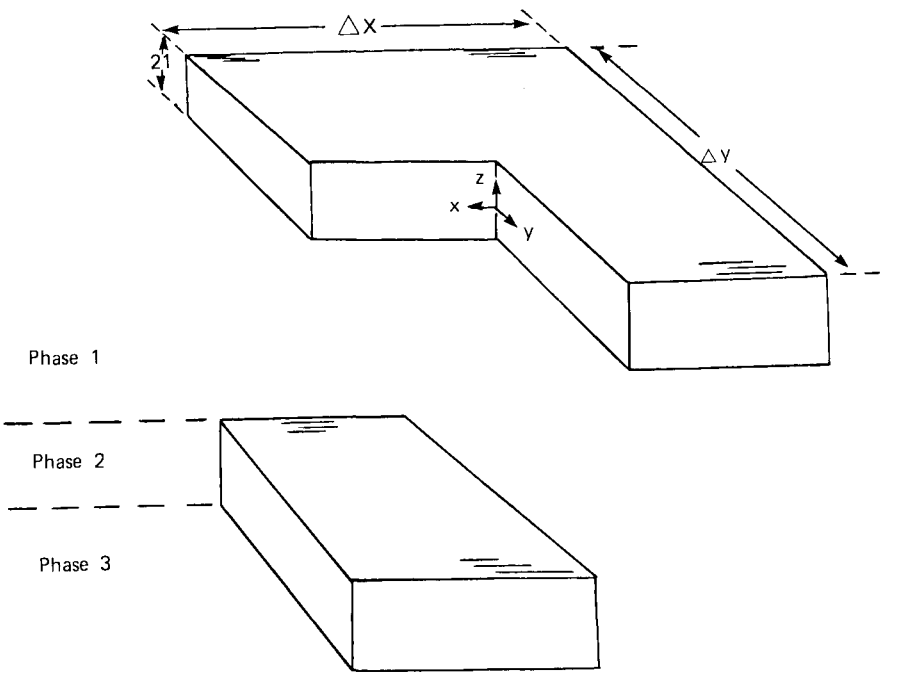

FIG. 1 Microscopic volume enclosing the interfacial region.

The interfacial region contains a large concentration of surfactant molecules such that the viscosity in the region is also large. Inertial momentum transfer, which is inevitably small within the very thin transition region, is then considered negligible compared to viscous momentum transfer.

A balance of the linear momentum on this fluid element may be written for the y component (see Fig. 2) as

$$\int_{-\ell}^{\ell} \left(\tau_{xy}\big|_{\Delta x} - \tau_{xy}\big|_{0} \right) \Delta y \, dz + \int_{-\ell}^{\ell} F_y \, \Delta x \, \Delta y \, dz + \int_{-\ell}^{\ell} \left(\tau_{yy}\big|_{\Delta y} - \tau_{yy}\big|_{0} \right) \Delta x \, dz + \left(\tau_{zy}\big|_{\ell} - \tau_{zy}\big|_{-\ell} \right) \Delta x \, \Delta y = 0 \tag{1}$$

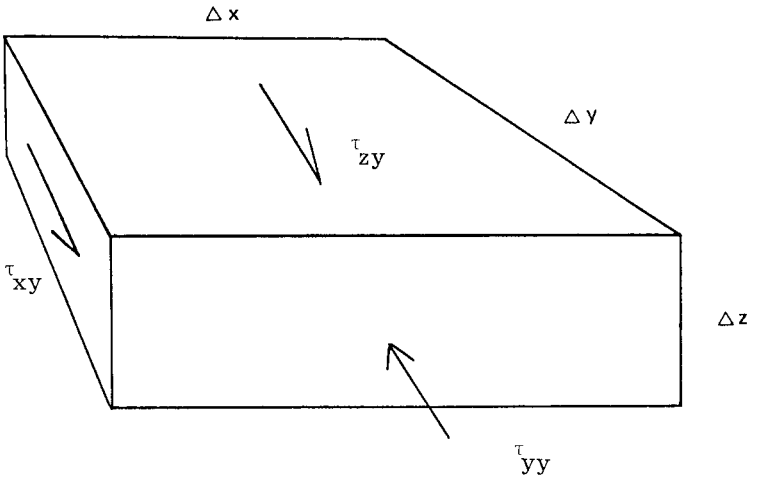

FIG. 2 Linear momentum transfer in the y direction for the microscopic interfacial volume.

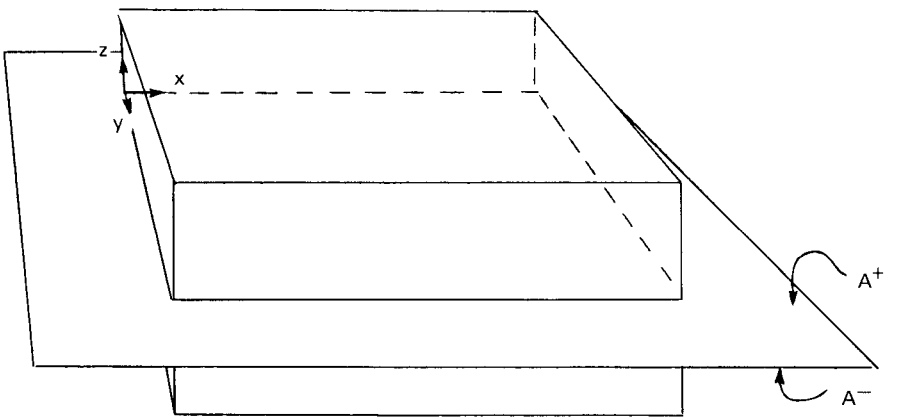

FIG. 3 Macroscopic "dividing surface" approach to the interfacial region.

Here τ_{xy}, τ_{yy}, and τ_{zy} are the contact stresses and F_y is the body force density in the y component containing both local and nonlocal force interactions.

However, most of our observations of the fluid-fluid interface occur at a much larger length scale then 2ℓ, for which the interfacial region appears to have virtually zero thickness. For this and other reasons it is often useful to model the statics and dynamics of the region as those of a singular "dividing surface."

Using this approach, the fluid element may be envisioned quite artificially, as in Fig. 3. We shall call this approach the "macroscopic approach." From the macroscopic approach, the properties of the bulk phases are assumed to possess the same values from the outer boundaries of the interfacial region up to the dividing surface, at which they generally possess singularities. The difference between the macroscopic approach and the true approach is depicted in Fig. 4.

The balance of the y component of linear momentum using the macroscopic approach to the surface becomes

$$\int_{-\ell}^{\ell} \left(\tau^{m}_{xy}\big|_{\Delta x} - \tau^{m}_{xy}\big|_{0} \right) \Delta y \, dz + \int_{-\ell}^{\ell} F^{m}_{y} \, \Delta x \, \Delta y \, dz$$

$$+ \int_{-\ell}^{\ell} \left(\tau^{m}_{yy}\big|_{\Delta y} - \tau^{m}_{yy}\big|_{0} \right) \Delta x \, dz$$

$$+ \left(\tau^{m1}_{zy}\big|_{\ell} - \tau^{m1}_{zy}\big|_{A+} \right) \Delta x \, \Delta y$$

$$+ \left(\tau^{m2}_{zy}\big|_{A-} - \tau^{m2}_{zy}\big|_{-\ell} \right) \Delta x \, \Delta y = 0 \tag{2}$$

where

$$\int_{-\ell}^{\ell} \left(\tau^{m}_{xy}\big|_{\Delta x} - \tau^{m}_{xy}\big|_{0} \right) \Delta y \, dz = \int_{-0}^{\ell} \left(\tau^{m1}_{xy}\big|_{\Delta x} - \tau^{m1}_{xy}\big|_{0} \right) \Delta y \, dz$$

$$+ \int_{-\ell}^{0} \left(\tau^{m2}_{xy}\big|_{\Delta x} - \tau^{m2}_{xy}\big|_{0} \right) \Delta y \, dz \tag{3}$$

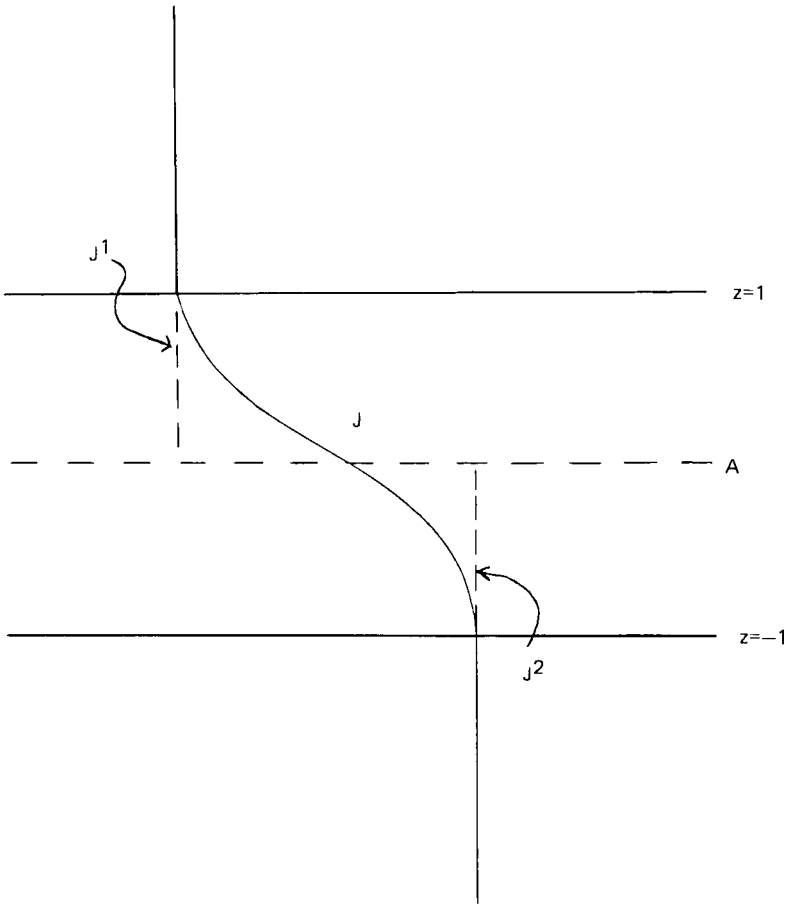

FIG. 4 Difference between the macroscopic and true approaches to the interface for a generic field quantity J.

and where m1 refers to the macroscopically perceived variable relative to phase 1 "at the surface," and similarly, m2 is with respect to phase 2.

What we wish to assign to our dividing surface is the difference between the artificial assessment of the linear momentum content of the element $\Delta x\ \Delta y\ \Delta z$ and the true linear momentum content. The resulting equation is the surface excess linear momentum equation. Subtracting Eq. (2) from Eq. (1) and dividing by the area element $\Delta x\ \Delta y$ yields

$$\int_{-\ell}^{\ell}\left(\frac{\tau_{xy}\,|_{\Delta x}-\tau_{xy}\,|_{0}}{\Delta x}-\frac{\tau^{m}_{xy}\,|_{\Delta x}-\tau^{m}_{xy}\,|_{0}}{\Delta x}\right)dz+\int_{-\ell}^{\ell}\left(F_y-F^{m}_{y}\right)dz$$

$$+\int_{-\ell}^{\ell}\left(\frac{\tau_{yy}\,|_{\Delta x}-\tau_{yy}\,|_{0}}{\Delta y}-\frac{\tau^{m}_{yy}\,|_{\Delta y}-\tau^{m}_{yy}\,|_{0}}{\Delta y}\right)dz$$

$$+\tau^{m1}_{zy}\,|_{A+}-\tau^{m2}_{zy}\,|_{A-}=0 \qquad (4)$$

where we have noted

$$\tau_{zy}\,|_{\ell}=\tau^{m1}_{zy}\,|_{\ell} \quad \text{and} \quad \tau_{zy}\,|_{\ell}=\tau^{m2}_{zy}\,|_{-\ell} \qquad (5)$$

Finally, taking the limit as

$$\Delta x\ \Delta y \to 0$$

we obtain

$$\frac{\partial}{\partial x}\int_{-\ell}^{\ell}\left(\tau_{xy}-\tau^{m}_{xy}\right)dz+\frac{\partial}{\partial y}\int_{-\ell}^{\ell}\left(\tau_{yy}-\tau^{m}_{yy}\right)dz$$

$$+\int_{-\ell}^{\ell}\left(F_y-F^{m}_{y}\right)dz=\left[\tau_{zy}\right] \qquad (6)$$

Where the "jump" in τ_{zy} is defined as

$$\left[\tau_{zy}\right]=\tau^{m2}_{zy}\,|_{A-}-\tau^{m1}_{zy}\,|_{A+} \qquad (7)$$

We may now define the surface excess pressure components as

$$\tau^{s}_{xy}\equiv\int_{-\ell}^{\ell}\left(\tau_{xy}-\tau^{m}_{xy}\right)dz \qquad (8a)$$

and

$$\tau^{s}_{yy} \equiv \int_{-\ell}^{\ell} \left(\tau_{yy} - \tau^{m}_{yy} \right) dz \tag{8b}$$

and the y component of the surface excess force density as

$$F^{s}_{y} \equiv \int_{-\ell}^{\ell} \left(F_{y} - F^{m}_{y} \right) dz \tag{8c}$$

so that the surface excess linear momentum equation for the y component of linear momentum becomes

$$F^{s}_{y} + \frac{\partial}{\partial x} \tau^{s}_{xy} + \frac{\partial}{\partial y} \tau^{s}_{yy} = [\tau_{zy}] \tag{9}$$

Similarly it may be shown that

$$F^{s}_{x} + \frac{\partial}{\partial x} \tau^{s}_{xx} + \frac{\partial}{\partial y} \tau^{s}_{yx} = [\tau_{zx}] \tag{10}$$

and

$$[\tau_{zz}] = 0 \tag{11}$$

Equations (9–11) are general surface excess stress equations for the planar fluid surface.

The Newtonian constitutive model for the pressure tensor τ_{jj}, where

$$\tau_{jj} = \begin{bmatrix} \tau_{xx} & \tau_{xy} & \tau_{xz} \\ \tau_{yx} & \tau_{yy} & \tau_{yz} \\ \tau_{zx} & \tau_{zy} & \tau_{zz} \end{bmatrix} \tag{12}$$

is given by

$$\tau_{ij} = \mu \Delta_{ij} - \left(\frac{2}{3}\mu - \kappa \right) v_{k,k} \delta_{ij} - p_t t^{a}_{i} t^{\beta}_{j} \delta_{a\beta} - p n^{n}_{i} n_{j} \tag{13}$$

Where p_t is the tangential component of the pressure, p the normal component, μ the shear viscosity, and κ the dilatational viscosity.

Here the rate of deformation tensor Δ_{ij} is given in cartesian coordinates as

$$\Delta_{ij} = \left(\frac{\partial v_i}{\partial x^j} + \frac{\partial v_j}{\partial x^i} \right) \tag{14}$$

where the summation convention is used over the indices i, j, as $i = 1,2,3$; $v_{k,k}$ is the divergence of the velocity v_k; δ_{ij} is the Kronecker delta; t_i^{δ} is the hybrid tensor of the surface, where α and β represent surface coordinates, as $\alpha = 1,2$; and n_i is the unit normal of the surface. From Eq. (13), then,

$$\tau_{xy} = \mu \left(\frac{\partial v_x}{\partial y} + \frac{\partial v_y}{\partial x} \right) \tag{15a}$$

and

$$\tau_{yy} = p_t + 2\mu \frac{\partial v_y}{\partial y} - \left(\frac{2}{3}\mu - \kappa \right) \left(\frac{\partial v_x}{\partial x} + \frac{\partial v_y}{\partial y} + \frac{\partial v_z}{\partial z} \right) \tag{15b}$$

Using Eq. (15) in Eq. (8), with the continuity of velocity conditions (see Ref. 6)

$$v_\alpha^{m1}(0) = v_\alpha^{m2}(0) = v_\alpha^s$$

and

$$v_z^{m1}(0) = v_z^{m2}(0) = 0 \tag{16}$$

the last of which is valid for small rates of mass transfer, provides

$$\tau_{xy}^s = \mu^s \left(\frac{\partial v_x^s}{\partial y} + \frac{\partial v_y^s}{\partial x} \right) \tag{17}$$

and

$$\tau_{yy}^s = \sigma + 2\mu^s \frac{\partial v_y^s}{\partial y} + (\kappa^s - \mu^s) \left(\frac{\partial v_x^s}{\partial x} + \frac{\partial v_y^s}{\partial y} \right) \tag{18}$$

where we have defined

$$\mu^s \equiv \int_{-\ell}^{\ell} (\mu - \mu^m)\, dz \tag{19}$$

as the surface excess shear viscosity,

$$\kappa^s \equiv \int_{-\ell}^{\ell} (\kappa - \kappa^m) dz + \frac{1}{3}\mu^s \tag{20}$$

as the surface excess dilatational viscosity, and

$$\sigma \equiv \int_{-\ell}^{\ell} (p^m - p_t) dz \tag{21}$$

as the surface tension.

Substituting Eqs. (17) and (18) into Eq. (9), we have an explicit relation between interfacial stress and deformation:

$$[\tau_{zy}] = F_y^s + \frac{\partial \sigma}{\partial y} + (\kappa^s + \mu^s) \frac{\partial}{\partial y} \frac{\partial v_x^s}{\partial x} + \frac{\partial v_y^s}{\partial y} - \mu^s \frac{\partial}{\partial x} \left(\frac{\partial v_x^s}{\partial y} - \frac{\partial v_y^s}{\partial x} \right) \tag{22}$$

Similarly, it may be shown from Eqs. (10) and (11) that

$$[\tau_{zz}] = F_x^s + \frac{\partial \sigma}{\partial x} + (\kappa^s + \mu^s) \frac{\partial}{\partial x} \left(\frac{\partial v_x^s}{\partial x} + \frac{\partial v_y^s}{\partial y} \right) + \mu^s \frac{\partial}{\partial y} \left(\frac{\partial v_x^s}{\partial y} - \frac{\partial v_y^s}{\partial x} \right) \tag{23}$$

and

$$[\tau_{xx}] = 0 \tag{24}$$

Interfacial stress behavior for the Newtonian surface is thus defined in terms of three stress coefficients μ^s, κ^s, and σ.

III. SURFACE DILATATIONAL PROPERTIES

Surface dilatational properties are those properties that are necessary to define fully a pure expansion or compression of a fluid surface. According to the Newtonian surface stress model (22–24), these properties may be identified as σ and κ^s.

This may clearly be seen by presenting Eqs. (22–24) in the more general vector form as follows. We let $\underline{i}_x$, $\underline{i}_y$, and $\underline{i}_z$ denote base vectors of a cartesian space, possessing the following tensor and differential properties:

$$\underline{\underline{I}} = \underline{i}_x \underline{i}_x + \underline{i}_y \underline{i}_y + \underline{i}_z \underline{i}_z \tag{25}$$

is the unit tensor of the cartesian space,

$$\underline{\underline{I}}_s = \underline{i}_x \underline{i}_x + \underline{i}_y \underline{i}_y \tag{26}$$

is the unit surface tensor of the surface A (with normal $\underline{i}_z$),

$$\nabla = \underline{i}_x \frac{\partial}{\partial x} + \underline{i}_y \frac{\partial}{\partial y} + \underline{i}_z \frac{\partial}{\partial z} \tag{27}$$

is the spatial gradient operator, and

$$\nabla_s = \underline{i}_x \frac{\partial}{\partial x} + \underline{i}_y \frac{\partial}{\partial y} \tag{28}$$

is the surface gradient operator.

Then Eqs. (22) to (24) may be expressed in the vector form

$$\underline{n} \cdot [\underline{\underline{P}}] = \nabla_s \cdot \underline{\underline{\Sigma}} \tag{29}$$

where $\underline{\underline{P}}$ is the bulk phase pressure tensor and $\underline{\underline{\Sigma}}$ is the surface tension tensor:

$$\underline{\underline{\Sigma}} = \sigma \underline{\underline{I}}_s + (\kappa^s - \mu^s) \nabla_s \cdot \underline{v}^s \underline{\underline{I}}_s + \mu^s \left(\nabla_s \underline{v}^s + \nabla_s \underline{v}^{s\dagger} \right) \tag{30}$$

For a purely expanding or compressing surface Eq. (30) becomes

$$\underline{\underline{\Sigma}} = \left(\sigma + \kappa^s \nabla_s \cdot \underline{v}^s \right) \underline{\underline{I}}_s \tag{31}$$

revealing the dilatational properties of the surface to be the surface tension σ and the surface dilatational viscosity κ^S.

Many of our results will be expressed in terms of a "dynamic" surface tension that is measured over a spherical fluid surface. Mathematically, the dynamic surface tension may be expressed as

$$\bar{\sigma} = \frac{1}{2} \underline{\underline{I}}_S : \underline{\underline{\Sigma}} \tag{32}$$

where (:) denotes the double scalar product operation. Using Eq. (31) in Eq. (32), we have that the dynamic surface tension is composed of both thermodynamic and viscous parts:

$$\bar{\sigma} = \sigma + \kappa^S \nabla_S \cdot \underline{v}^S \tag{33}$$

Identifying the reversible and irreversible contributions to the dynamic surface tension is a difficult and open question. Numerous attempts have been made, including postulating the functionality of $\bar{\sigma}$ upon surfactant mass transfer [7–9], assuming negligible surface tension gradient (zeroth-order solution) [10], or defining the apparent dissipation in $\bar{\sigma}$ as the viscous, irreversible contribution [11–15]. The particular difficulty with the latter approach, as we will discuss, is that much of the observed "dissipation" in the dynamic surface tension is reversible energy transfer between surface and bulk phases. The former approaches, although apparently more rational, do not guarantee that the measured "viscous" contribution (κ^S) is not a "parameter" of the mass transfer model, rather than a true viscosity.

Still another class of techniques has been proposed based on the propagation of thermally induced microscopic capillary waves in the interface [16–19]. However, such techniques raise the fundamental question of whether microscopic capillary waves may be modeled by means of a macroscopic capillary wave theory.

In the present work we do not speculate on the contributions to the dynamic surface tension but rather, investigate the directly measured dynamic tension $\bar{\sigma}$ and the dilatational modulus

$$E^* \equiv - \frac{d\bar{\sigma}}{d \ln A} \tag{34}$$

which measures the change in tension with surface area expansion. The dilatational modulus is a very important measure of dilatational surface stress as it expresses in a certain sense the gradient of

dynamic surface tension. It is, of course, the gradient of dynamic surface tension that plays a direct role in the surface stress equations [see Eqs. (22) and (23)].

The several techniques that have been proposed to measure the surface dilatational viscous effect implicit in Eq. (33) on the basis of dissipation or phase lag measurements [11–15] have done so by transforming the dilatational modulus [34] into the complex plane, where the imaginary contribution to the modulus is defined as arising from a surface viscous mechanism.

Lucassen and van den Tempel [11,12] and Djabbarah and Wasan [13] measured wave properties of a mechanically driven longitudinal surface wave. In the analysis of the wave motion, the amplitude of the wave ξ was expressed naturally in the complex plane, such that

$$\frac{\partial \sigma}{\partial x} = E^* \frac{\partial^2 \xi}{\partial x^2}$$

defines the complex dilatational modulus, where

$$E^* = E' + i\omega\eta$$

The real portion E' is called the surface elasticity and the term η is called the surface dilatational viscosity, where ω is the wave frequency.

A similar treatment has been used by Rambhadran et al. [14], who measured the pressure drop across an oscillating droplet to determine the surface elasticity and dilatational viscosity.

A technique proposed by Clint et al. [15] is based on the same interpretation of the dilatational modulus. A droplet is formed on the tip of a capillary. In a brief instant the droplet is expanded to a new radius and the pressure drop over the droplet is then measured as a function of time at a fixed radius. The dilatational modulus, which may be inferred directly from the pressure versus time trace, is then transformed into the imaginary plane using a Fourier analysis, and the definition of real and imaginary parts, as with the damped wave and oscillating droplet experiments, allows the determination of the surface dilatational viscosity.

It is, however, not at all clear that the surface dilatational viscosity determined in this way is in fact the parameter defined in Eq. (33) as the surface dilatational viscosity. In fact, the damping quantified by the complex contribution to the dilatational modulus is controlled in part by an exchange of surfactant between the surface and bulk phases, which is not a dissipative mechanism.

IV. APPLICATIONS

A. Foam Rheology

As an application of surface dilatational properties, we may consider the rheology of a "wet" foam, or a foam with a small gas volume fraction. Because of the presence of gas phase, foam flow may often be accompanied by a significant dissipation of energy due to compression or expansion of the gas phase. This dissipation of energy is quantified in the Newtonian constitutive model with the lesser known "dilatational" viscosity κ.

Much effort has been given to the measurement of this second coefficient of viscosity for pure fluids [20–24] and has revealed that the dilatational viscosity is generally larger than the shear viscosity. Still, since most pure fluid viscous flow displays a small degree of compressibility, the dilatational viscosity of pure fluids is primarily of academic interest.

However, the degree of compressibility possible in foam flow makes the effective dilatational viscosity of a foam of general practical interest.

The first theoretical calculation of the dilatational viscosity of a wet foam was made by Taylor [25], who derived the following relation for a dilute wet foam containing spherical bubbles:

$$\kappa^* = \frac{4\mu}{3\phi} \tag{35}$$

where the asterick denotes effective foam properties. Here μ is the liquid phase shear viscosity and ϕ is the gas volume fraction.

Prud'homme and Bird [26] extended the result of Taylor to first order in ϕ with the relation

$$\kappa^* = \frac{4\mu}{3\phi}(1 - \phi) \tag{36}$$

Recently, we extended this result to include surface rheological effects [27] as

$$\kappa^* = \frac{4\mu}{3\phi}\left(1 - \phi + \frac{\kappa^S}{\mu a}\right) \tag{37}$$

where κ^S is the surface dilatational viscosity and a is the bubble radius.

It is certainly not surprising that the dilatational viscosity of a foam would be directly related to the dilatational viscosity of individual surfaces within that foam. In fact, as one would expect, as

liquid is removed from the foam (this limit must be taken in a qualitative sense) the single remaining source of the foam dilatational viscosity is the surface dilatational viscosity.

A relevant application of the surface dilatational viscosity through the effective foam dilatational viscosity Eq. (37) may be found in the process of foam flow in porous media in the presense of oil (i.e., EOR).

Dilatation (compression or expansion) in EOR may occur by several mechanisms, among which are:

1. Absolute pressure changes as foam flows from high-pressure to low-pressure zones in the porous medium result in an expansion of the foam.
2. Contact of foam with oil phase may result in a rapid expansion of the foam due to surface instability.
3. Geometrical nonuniformities in the capillary geometry (e.g., expansion/compression in the capillary diameter) may result in expansion/compression of the foam.
4. Gas transfer from smaller to larger bubbles results in a dilatation of the foam.

A simple model may be proposed by which these dilatational effects in EOR may be gauged in significance relative to shearing effects. In Fig. 5 we show a cross section of a fully formed foam structure of uniform bubble size flowing through a smooth capillary with an assumed Poiseuilleian profile as a model of foam flow through microscopic (generally nonuniform) capillaries within a porous medium. The bubbles are allowed to oscillate with a definite frequency about a mean radius to simulate the effect of dilatation caused by mechansims such as those discussed above.

The dissipation of energy due to the shear viscosity of the foam and the dissipation of energy due to the dilatational viscosity of the foam may be compared for specific values of the capillary radius, bubble size, frequency, and so on, to estimate the significance of the dilatational effect.

The dissipation of energy due to the shear viscosity of the foam may be estimated by the Poiseuille relation

$$\varepsilon_{\mu}^{*} = \frac{(\Delta p/L)^2 R^2}{8\mu^{*}} \tag{38}$$

where $\Delta p/L$ is the pressure drop over the capillary and R is the capillary radius.

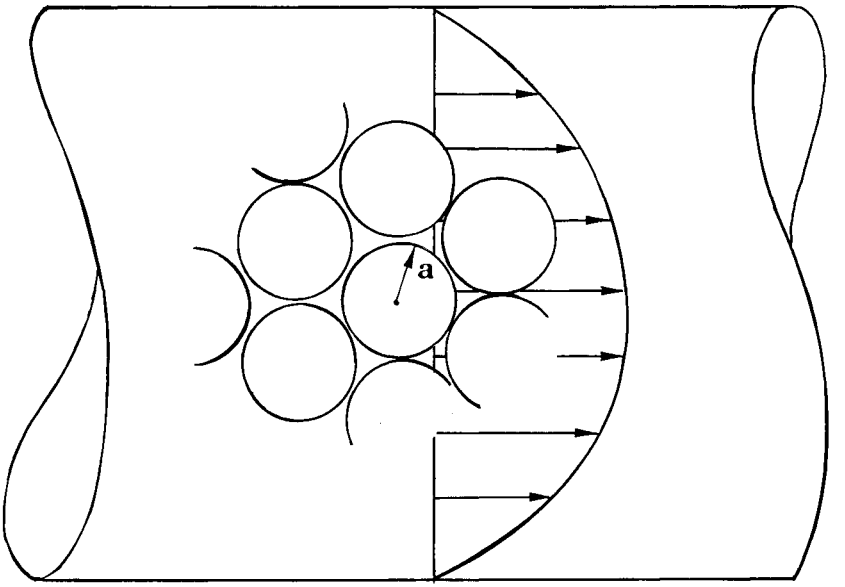

FIG. 5 Cross section of a foam with oscillating bubble surfaces flowing within a smooth capillary.

The dissipation of energy due to the dilatational viscosity of the foam may be approximated as

$$\varepsilon_{\kappa} \simeq \kappa^{*} \omega^{2}$$

As physical constants we choose for the capillary radius R a value of 10 μm, for the pressure drop 10 psi/ft, for the mean bubble radius 1 μm, for the foam shear viscosity 100 cP, for the dilatational viscosity of the foam as $\kappa^{*} \simeq (4/3)(\kappa^{S}/a)$ and conservatively for the frequency of surface expansion 2 Hz. For this particular geometry, then,

$$\frac{\varepsilon_{\kappa}^{*}}{\varepsilon_{\mu}^{*}} \simeq \kappa^{S} \times 10^{3} \tag{39}$$

where κ^{S} has the units of sP. As mentioned previously, much work remains to establish the absolute magnitude of κ^{S}, but the work to

date indicates that the surface dilatational viscosity is larger in general than the surface shear viscosity and may often approach a value of 1 sP [7–9]. Given the qualitative nature of this model calculation, at most one can speculate that dilatational effects are comparable in significance to shearing effects in the EOR process.

B. Enhanced Oil Recovery

To determine experimentally the significance of surface dilatational properties in EOR, we have performed oil displacement experiments in Berea sandstone cores using aqueous foams stabilized by straight-chain α-olefin sulfonates. Saturation profiles were determined using both microwave and gamma-ray absorption techniques. (A complete discussion of the microwave and gamma-ray experiments together with the results summarized here may be found in Ref. 28.)

The Berea cores (4 in. x 0.75 in. x 12 in.) used as porous media were vacuumed to displace interstitial air and then saturated with 1% NaCl aqueous solution. About six pore volumes of the same solution was injected to stabilize the clay as well as to determine the absolute permeability and porosity (average permeability = 380 millidarcy, average porosity = 0.19). The porous medium was then flooded with Salem crude oil (viscosity at room temperature = 6cP) to irreducible water content. Waterflood (1% NaCl) was injected into the porous medium until the rock adsorption was completed.

Two types of displacement experiments were conducted to analyze foam behavior in porous media. In one set of experiments nitrogen gas was injected following the surfactant solution to form the foam in situ with an imposed pressure differential of 45 psi. In the second set of experiments the nitrogen gas was injected at a constant flow rate of 10 ft/day. During the constant flow rate experiments the dynamic fluid saturations along the core length were measured by the combined gamma ray/microwave technique.

Table 1 shows the results of the foam-enhanced oil recovery tests for the constant-pressure and the constant-flow-rate experiments, respectively. The foam-enhanced oil recovery results from both sets of experiments are similar in that the recovery efficiency and gas breakthrough time increased in the same order: C_{12} AOS, C_{14} AOS, and C_{16} AOS.

On the basis of these experiments and the discussion of Section IV. A, one would expect the dilatational viscosity of the C_{16} AOS-stabilized surface to be the largest, followed by C_{14} AOS and then C_{12} AOS (since large foam viscosity results in a lower foam mobility and generally a higher oil displacement efficiency).

As discussed previously [see Eqs. (33) and (34)], the dilatational modulus, which is a directly measurable quantity, contains not only

TABLE 1 Saturation Data for Constant-Pressure and Constant-Flow-Rate Experiments

	Under constant pressure			Under constant flow rate		
Experiment:	1	2	3	4	5	6
	C_{12}	C_{14}	C_{16}	C_{12}	C_{14}	C_{16}
Initial oil saturation	73.0	71.5	74.0	74.0	73.8	75.2
Waterflood oil saturation	42.1	39.8	41.5	42.1	43.2	43.5
Surfactant flood oil saturation	39.0	37.0	39.5	39.8	40.6	41.7
Percent recovery[a]	4.3	3.9	2.7	3.1	3.5	2.4
Foam-flood oil saturation	28.5	22.5	23.5	33.9	33.1	30.6
Percent recovery[a]	14.4	20.2	21.6	8.0	10.2	14.8
Breakthrough time (min)	23.0	35.0	39.0	36.0	48.0	62.0

[a]Percent oil recovery is based on the initial oil saturation.

the surface dilatational viscosity effect but also the surface tension gradient effect, which might also be considered very relevant to foam mobility in EOR.

We have recently developed a method for measuring dynamic surface tension and the dilatational modulus based on the maximum bubble pressure technique for surface tension measurement. The experiment is discussed in detail elsewhere [29]. Also, see the work of Mysels [43].

Using this technique, we have measured the dilatational modulus for the three straight-chain α-olefin sulfonate systems used in the foam-flooding experiments (see Fig. 6).

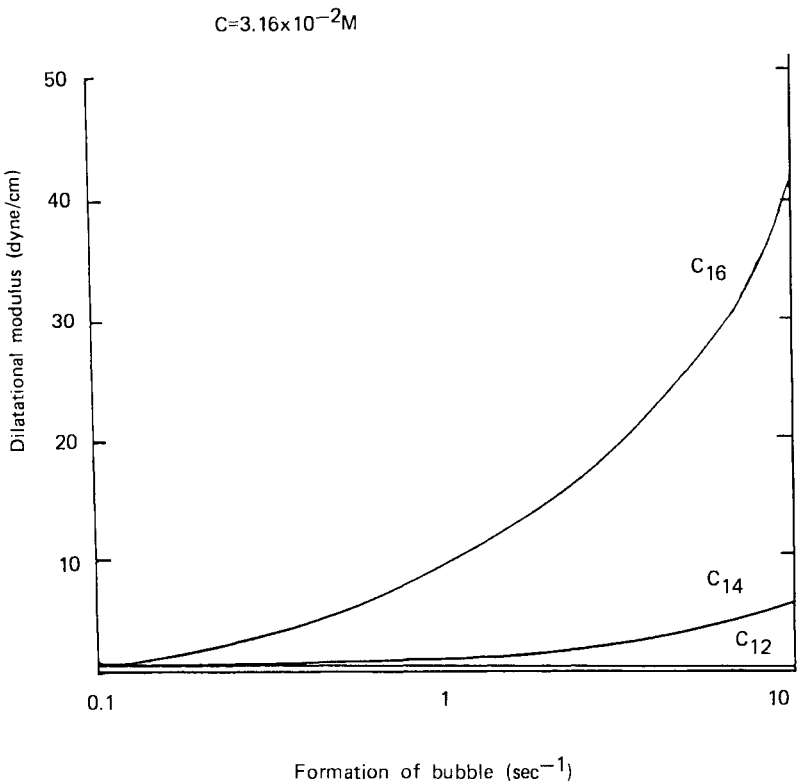

FIG. 6 Dilatational modulus versus frequency of surface expansion for C_{12}AOS, C_{14}AOS, and C_{16}AOS surfaces.

The results show that the largest dilatational modulus is that of the C_{16}AOS system, followed by C_{14}AOS and C_{12}AOS, the exact order suggested by the core-saturation experiments, indirectly confirming the significance of dilatational surface properties in EOR.

The significance of the dynamic surface tension gradient in EOR has been confirmed by Hirasaki and Lawson [30], who concluded that the apparent viscosity of a foam flowing through smooth capillaries in a porous medium increases with increasing surface tension gradient. The increasing foam viscosity results in a low foam mobility and therefore a greater oil displacement efficiency.

However, most of the research to date concerning the role of surface tension and viscosities in EOR has focused on the oil-water interface rather than the gas-water surface. Slattery [31] has concluded, based on a qualitative model of dynamic interfacial effects in EOR, that for low-tension systems, decreasing interfacial viscosity may significantly increase oil displacement, although Flumerfeldt et al. [32] have since concluded that the interfacial viscous effect is a smaller-order contribution than the effect of interfacial tension. In any case, the desirability of a low interfacial tension in EOR appears to be unanimous [31-35].

C. Foam Stability

The efficiency of oil displacement by aqueous foams stabilized by the straight-chain α-olefin sulfonates suggests a further correlation between foam stability and the dilatational modulus. Such a correlation is justified by theoretical studies of thin foam film drainage and stability.

Since the original work of Reynolds [36], who determined the drainage of a liquid film between two flat immobile surfaces, both theoretical and experimental research has shown that drainage between two foam surfaces is generally much more rapid due in part to a fluidic mobility within the bounding surfaces of the film. In fact, much of the thin-film drainage research in the past three decades has focused on quantifying the relevant parameters within a thin film which determine whether the film will drain rapidly (promote instability of the foam) or slowly (promote stability), largely on the basis of the mobility of the bounding surfaces.

Johannes and Whitaker [37] investigated the gravitational thinning of a foam film stabilized by surface-active agents. Comparing both theoretical and experimental results, they concluded that an important foam stabilizing mechanism is a large dilatational modulus, or in their terms, either a large surface dilatational viscosity or a large surface tension gradient. [Note again the difficulty in distinguishing between the source terms in Eq. (33).]

More recently, Zapryanov et al. [38] have concluded that the interfacial tension gradient is a governing factor in determining whether a film drains as an immobile or a mobile bounded film. They predict that at high interfacial tension gradient the film drains according to the Reynolds model, while at low interfacial tension gradient the film becomes significantly effected by parameters such as interfacial viscosity (sum of μ^S and κ^S). This result is illustrated in Fig. 7 where the draining rate of an emulsion film is predicted as a function of the interfacial tension gradient ($K_\sigma = -\partial\sigma/\partial C$, where C is the bulk-phase surfactant concentration) and interfacial viscosity. The dilatational modulus has also been shown significant to foam film stability, emulsion stability [39], and the stability of a liquid film on a solid surface [40]. For a more complete review of thin-film studies, see Ref. 3.

To confirm the significance of the dilatational modulus on foam stability and to show the direct relation to the thin-film drainage, both drainage and foam stability tests were performed for the three surfactant-stabilized aqueous foams C_{12}AOS, C_{14}AOS, and C_{16}AOS [41]. The drainage time of the foam films was studied using the

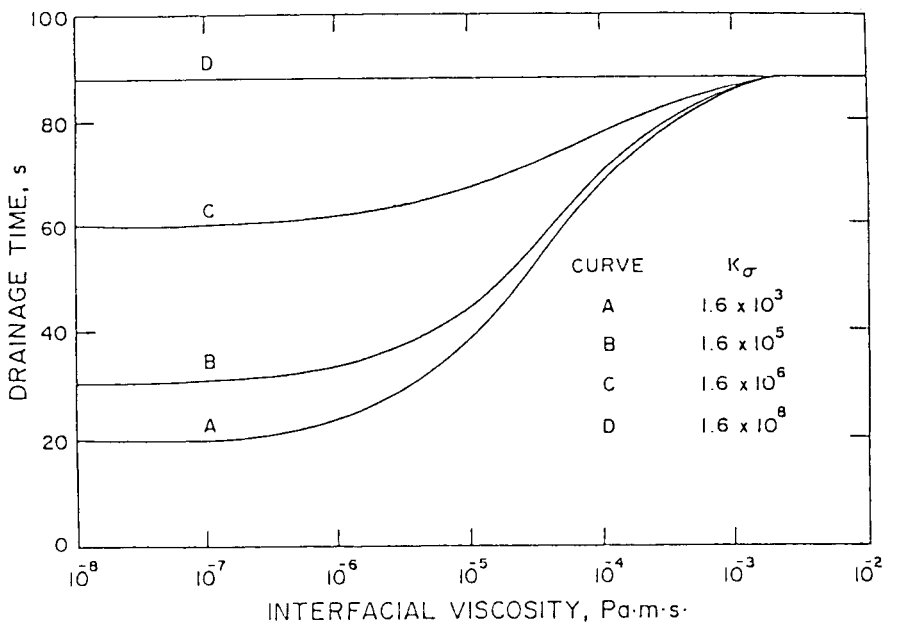

FIG. 7 Effect of interfacial viscosity and interfacial tension gradient on thin-film drainage time. (From Ref. 38.)

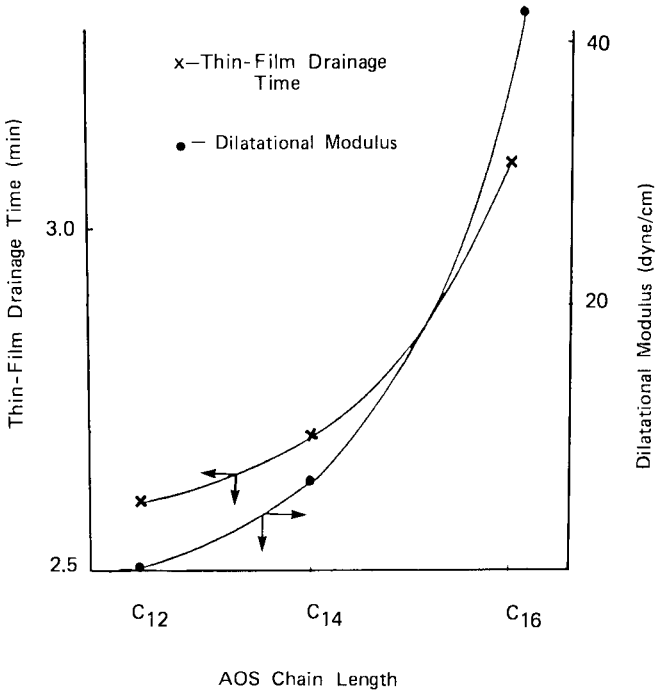

FIG. 8 Thin-film drainage time versus dilatational modulus.

interference microscopic technique described in Ref. 42. Thin films of any desired radius are formed in a specially designed glass cell containing a double concave meniscus. Monochromatic light (wavelength of 546.1 nm) is exposed to the draining film and the reflected light is measured by a fiber-optic probe. As the film thins, the variable thickness produces a series of interference patterns which are recorded through the fiber-optic probe upon a strip-chart recorder. The values of the photocurrent versus time enable an estimation of both the thinning rate and the thickness of the film. To prevent evaporation the films were formed in a completely closed cell and sufficient time was allowed to saturate the cell atmosphere.

Figure 8 reveals the results of the drainage tests, illustrating the proportionality between the dilatational modulus and drainage time of the foam film. The drainage time is seen to increase with the identical order of surfactants as the order of increasing oil displacement in EOR, C_{12}AOS, C_{14}AOS, and C_{16}AOS. The foam stability tests were performed using both static and dynamic methods. The

static method entails foam generation in a graduated cylinder by shaking the cylinder and then monitoring the foam height with time. The foam half-life is determined by the first-order rate equation

$$-\frac{dV_f}{dt} = K_f V_f$$

where V_f is the foam volume and K_f the rate constant. The half-life $t_{1/2}$ is given by

$$t_{1/2} = \frac{0.693}{K_f}$$

The dynamic method is to produce uniform size bubbles at the end of a capillary immersed in a surfactant solution. The bubbles rise to the top of the solution and form a foam that with time reaches an equilibrium level.

In Fig. 9 the results of the static and dynamic foam stability test are plotted versus a dilatational modulus revealing a correlation with the film drainage measurements as foam stability is seen to increase with increasing dilatational modulus.

D. Emulsion Stability

Due to the analogous nature of emulsion stability phenomena to foam stability phenomena, it may be expected that the dilatational modulus also possesses a strong relevance to emulsion stability. To confirm this relevance, we have conducted emulsion stability experiments on oil-in-water emulsions with dodecane as the oil phase and 1 wt% sodium alkylnapthalene dissolved within the aqueous phase. The systems were varied with the addition of 2.5mM calcium chloride and/or 2 wt% gelatin within the aqueous phase.

The emulsion stability tests were conducted using a photomicrographic technique. The emulsion is placed within a Howard cell and photographed through a Nikon microscope with a magnification of 400× . The microscope has a maximum magnification of 1000× and is equipped with interference phase contrast, polarizing light, and slow and fast-speed cinematographic equipment.

The first photographs were taken 20 s after the sample had been emulsified. Additional photographs were taken over a 24-h period. The droplet size distribution was determined using a Zeiss MOP image analyzer. The size distribution was used to determine a first-

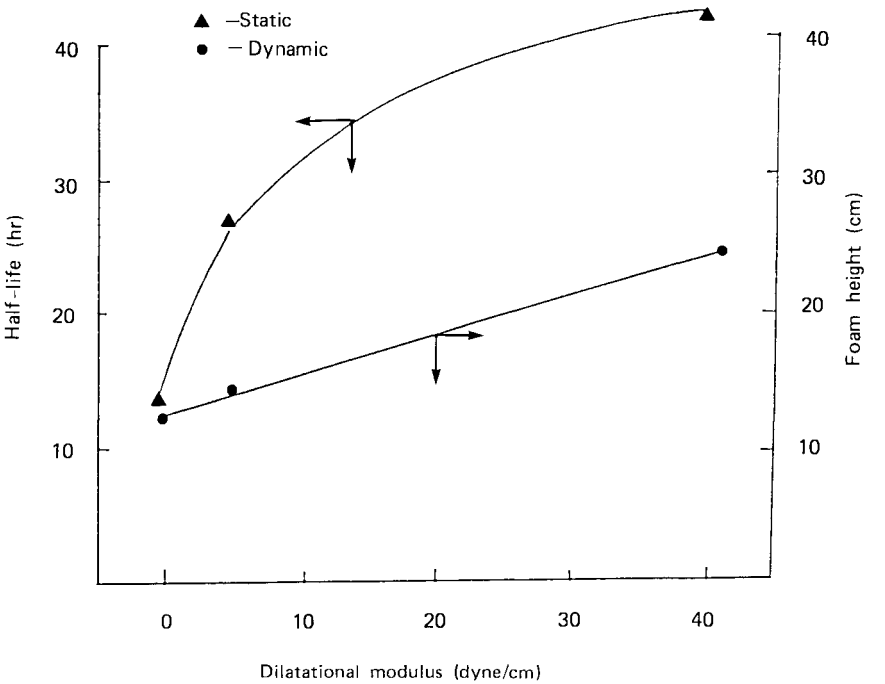

FIG. 9 Foam half-life and equilibrium foam height versus dilatational modulus.

order rate constant K where

$$N = N_0 \exp(-Kt)$$

Here N is the number density of droplets at time t and N_0 is the initial droplet number density.

In Table 2 the rate constants are given for the four emulsion systems. The constants reveal the gelatin to be a stabilizing component and the calcium salt to be a destabilizing component. In Fig. 10 the dilatational moduli of the four systems are plotted, showing the identical correlation observed with the foam systems. The larger the dilatational modulus of the oil/water interface, the greater the stability of the emulsion.

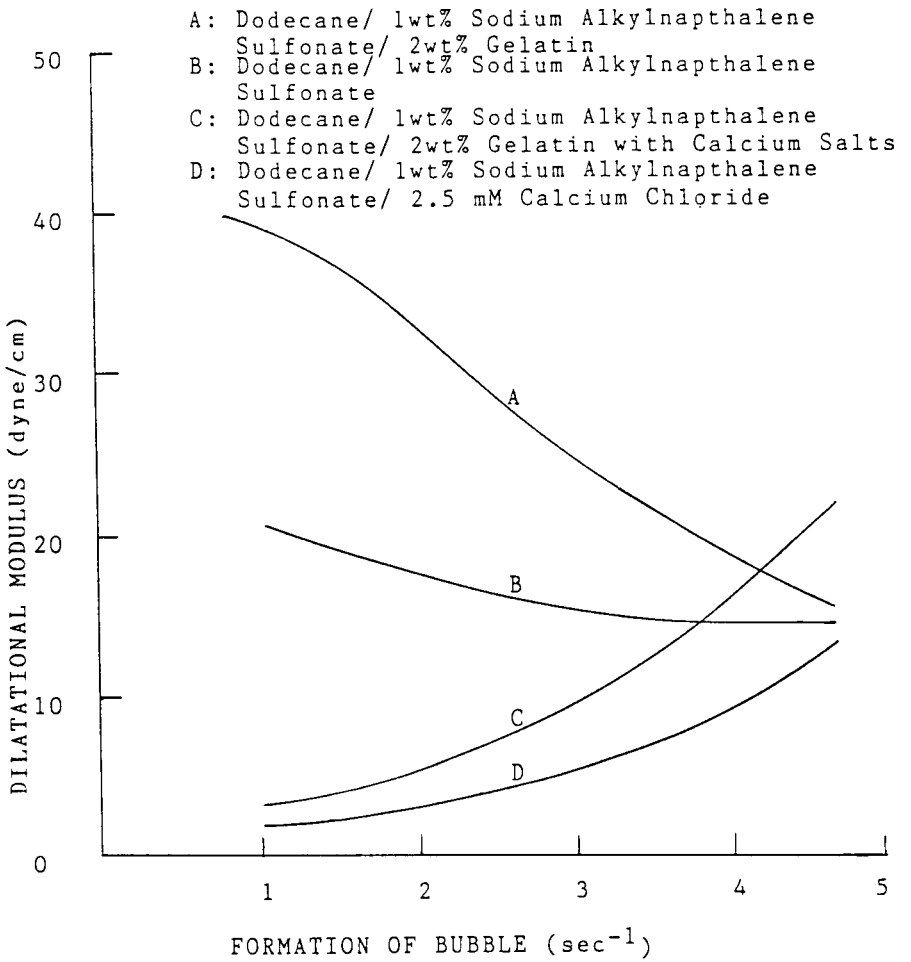

FIG. 10 Dilatational modulus versus frequency of bubble creation for four oil-water interfaces.

IV. SUMMARY

Dilatational surface properties arising from the presence of surface-active agents at the fluid/fluid interface may have both a thermodynamic (σ) and a viscous (κ^s) origin. The dilatational modulus [Eq. (34)] (or dynamic surface tension gradient) contains both the thermodynamic and viscous contributions, is directly measurable, and

TABLE 2 Coalescence Rate Data for the Water-in-Oil Emulsions

System	Rate constant (h^{-1})
A: Dodecane/1 wt% sodium alkylnapthalene sulfonate/2 wt% gelatin	~ 0.0
B: Dodecane/1 wt% sodium alkylnapthalene sulfonate	3.3×10^{-2}
C: Dodecane/1 wt% sodium alkylnapthalene sulfonate/2 wt% gelatin with calcium salts	8.7×10^{-2}
D: Dodecane/1 wt% sodium alkylnapthalene sulfonate/2.5 mM calcium chloride	1.1×10^{-1}

is significant to foam rheology, foam stability, emulsion stability, and oil displacement by foam flooding in porous media. Results presented indicate that a large dilatational modulus enhances foam stability, emulsion stability, and oil displacement in the foam-flooding EOR process. We are currently extending this research to conduct a systematic investigation of the dilatational modulus, including the effects of temperature, electrolyte, surfactant structure, and bulk phase, as well as an investigation of the significance of the dilatational modulus to other dynamic interfacial phenomena.

ACKNOWLEDGMENTS

The financial support provided by the National Science Foundation and the Department of Energy is gratefully acknowledged.

REFERENCES

1. M. Joly, in *Surface and Colloid Science*, Vol. V (E. Matijevic, ed.), Wiley Interscience, New York, 1962.
2. F. C. Goodrich in *Solution Chemistry of Surfactants*, Vol. 2 (K. L. Mittal, ed.), Academic Press, New York, 1979, p. 733.
3. A. K. Maholtra and D. T. Wasan, in *Thin Liquid Films*, Marcel Dekker, New York, in press.

4. D. A. Edwards and D. T. Wasan, submitted to J. Rheol. (1986).

5. D. A. Edwards and D. T. Wasan, submitted to J. Rheol. (1987).

6. D. A. Edwards and D. T. Wasan, submitted to J. Rheol. (1987).

7. K. Miyano, B. M. Abraham, L. Ting, and D. T. Wasan, J. Colloid Interface Sci., *92*:297 (1983).

8. L. Ting, D. T. Wasan, K. Miyano, and S. Q. Xu, J. Colloid Interface Sci., *102*:248 (1984).

9. L. Ting, D. T. Wasan, and K. Miyano, J. Colloid Interface Sci., *107*:345 (1985).

10. L. Wei, W. Schmidt, and J. C. Slattery, J. Colloid Interface Sci., *48*:1 (1974).

11. J. Lucassen and M. van den Tempel, J. Colloid Interface Sci., *41*:491 (1972).

12. J. Lucassen and M. van den Tempel, Chem. Eng. Sci., *27*:1283 (1972).

13. N. F. Djabbarah and D. T. Wasan, Chem. Eng. Sci., *37*:175 (1982).

14. T. E. Rambhadran, C. H. Byers, and J. C. Friendly, AIChE J., *22*:872 (1976).

15. J. H. Clint, E. L. Neustadter, and T. J. Jones, paper presented at the 2nd European EOR Symposium, 1985.

16. S. Hard and H. Lofgren, J. Colloid Interface Sci., *60*:529 (1977).

17. D. Byrne and J. C. Earnshaw, J. Phys. D: Appl. Phys., *12*:1145 (1979).

18. S. Hard and R. Neuman, J. Colloid Interface Sci., *82*:315 (1981).

19. S. Hard and R. Neuman, J. Colloid Interface Sci., *82*:315 (1981).

20. E. F. Fox and G. D. Rock, Phys. Rev. *70*:68 (1946).

21. L. N. Liebermann, Phys. Rev. *75*:1415 (1949).

22. L. Tisza, Phys. Rev., *61*:531 (1942).

23. J. Quinn, J. Acoust. Soc. Am., *18*:185 (1946).

24. S. B. Gurevich, C. R. U.S.S.R., *55*:17 (1947).

25. G. I. Taylor, Proc. R. Soc. London Ser. A, *226*:34 (1954).

26. R. K. Prud'homme and R. B. Bird, J. Non-Newt. Fluid Mech., *3*:261 (1977).

27. D. A. Edwards, H. Brenner, and D. T. Wasan, manuscript in preparation.

28. D. W. Huang, Ph.D. thesis, Illinois Institute of Technology, 1985.

29. R. Kao, A. Nikolov, D. A. Edwards, and D. T. Wasan, manuscript in preparation.

30. G. J. Hirasaki and J. B. Lawson, paper presented at the 58th Annual SPE Technical Conference, San Fransisco, 1983.

31. J. C. Slattery, AIChE J., *20*:1145 (1974).

32. R. W. Flumerfeldt, J. P. Oppenheim, and J. R. Son, AIChE Symp. Ser., *78*:113 (1982).

33. J. C. Melrose, Can. J. Chem. Eng., *48*:638 (1970).

34. O. R. Wagner and R. O. Leach, Soc. Pet. Eng. J., *6*:335 (1966).

35. D. T. Wasan, S. M. Shah, N. Aderangi, M. S. Chan, and J. J. McNamara, Soc. Pet. Eng. J., *18*:409 (1978).

36. O. Reynolds, Philos. Trans. R. Soc. London Ser. A, *77*:157 (1886).

37. W. Johannes and S. Whitaker, J. Phys. Chem., *69*:1471 (1965).

38. Z. Zapryanov, A. K. Maholtra, N. Aderangi, and D. T. Wasan, Int. J. Multiphase Flow, *9*:105 (1983).

39. J. Lucassen, M. van den Tempel, A. Vrij, and F. T. Hesselink, Proc. K. Ned. Akad. Wet., *B73*:108 (1970).

40. E. Ruckenstein and R. Jain, J. Chem. Soc. Faraday Trans. 2, *70*:132 (1974).

41. D. W. Huang, A. Nikolov, and D. T. Wasan, Langmuir, *2*:672 (1986).

42. A. A. Rao, D. T. Wasan, and E. D. Manev, Chem. Eng. Commun., *15*:63 (1982).

43. K. J. Mysels, Langmuir, 2:428 (1986).

2

The Effect of Surface-Active Agents in Distillation Processes

JOHN C. BERG *University of Washington, Seattle, Washington*

I. INTRODUCTION

Distillation is a complex vapor-liquid contacting operation involving large interfacial area-to-volume ratios. It is therefore not surprising that surface-active agents, whose characteristic feature is their ability to concentrate themselves at interfaces, should have the potential for profoundly influencing distillation. The literature contains ample evidence of such influence, but the subject is rarely examined in a systematic way. There are three major reasons for this. First, the consequences of the presence of surfactants in distillation can be

extremely varied and complex, manifesting themselves in such completely different ways in different circumstances that it is difficult to identify them as arising from a common origin. On the one hand, their presence may lead to the foam flooding of a column, rendering it totally inoperable. On the other hand, it has been shown how additions of surfactant may nearly double the efficiency of a packed tower [1] and significantly enhance the efficiency of a tray tower [2]. Second, the unraveling of the explanations of the effects of surfactants relies on the relatively new subject of interfacial hydrodynamics. Until relatively recently, the underlying principles of this discipline were not widely understood or appreciated. Indeed, the subject is in a state of evolution as ongoing basic research is bringing new insights. The topic is missing entirely from most books on hydrodynamics or fluid mechanics. Finally, the effects of surfactants are greatest in smaller-scale equipment, so the economic incentive for understanding them is not as great as it might otherwise be.

The motivation for an examination of the effects of surfactants on distillation at this time is twofold. First, there are situations for which sufficient understanding exists that practical advantage may be taken of efficiency-enhancing surfactant addition, or so that, on the other hand, surfactant-induced problems may be properly diagnosed. Second, the present state of knowledge concerning surfactant effects is highly incomplete. A review at this time, pointing out some of the present gaps, may stimulate further research.

In order to describe the observed effects of surfactants in distillation it is necessary to begin with a brief description of the distillation process itself. Next is given a discussion of interfacial and capillary phenomena in distillation in the absence of surfactants. This forms the basis for understanding the consequences of the presence of surfactants. Finally, the role of surfactants is discussed, and recommendations for further study are given.

II. THE DISTILLATION PROCESS

The objective of distillation is the separation or partial separation of the components of a liquid mixture by means of partial vaporization. It is necessary, of course, that the equilibrium composition of the vapor mixture differ from that of the liquid. In a single-stage continuous distillation in which a given liquid mixture is fed to a chamber where a given fraction is vaporized and separated from the liquid, it is the thermodynamic vapor-liquid equilibrium that dictates the extent of separation achievable. The degree of separation may be increased by connecting such single-stage units in series with countercurrent flow of the vapor and liquid. These "stages" are connected vertic-

ally in order to exploit gravity for phase disengagement. The result is a distillation "column," as shown schematically in Fig. 1. Heat is generally supplied only at the bottom, where the liquid is partially vaporized and sent up through the column. At the top, some of the vapor is condensed into liquid (called reflux) and sent back down the column, while the rest is removed as "overhead product." Feed may enter at any stage along the column. Separation of the more volatile from the less volatile components is achieved during the contact of the rising vapor with the descending reflux. On any given stage in the column, part of the vapor stream is condensed and part of the reflux stream is vaporized. The result of this exchange of (mostly latent) heat and mass between the streams is that the vapor stream emerging is enriched in the more volatile components, while the reflux liquid descending has been partially depleted of these components. Under conditions of ideal contact, the vapor and liquid streams emerging from a given stage are in equilibrium, but under no conditions can the streams being contacted on a given stage be

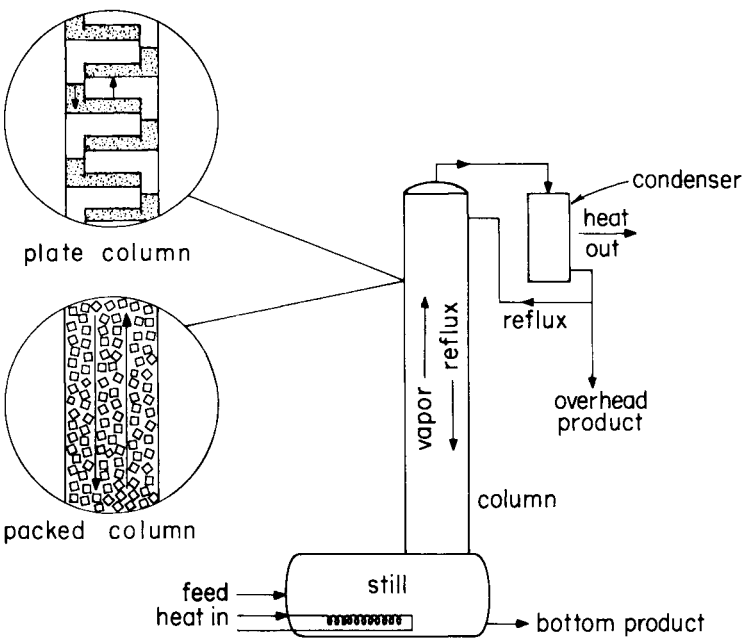

FIG. 1 Schematic of distillation equipment. Insets show a plate column (unsupported-area) and packed column (supported-area) configurations.

in equilibrium. There is thus a mass transfer driving force for the desired exchange of components between the streams. More details on the principles of multistage distillation may be found in a variety of textbooks [3–5].

A wide variety of equipment exists for carrying out distillation. Columns vary in size from heights as small as 100mm and diameters as small as 10mm, for bench-scale separations, up to giant columns with heights greater than 100m and diameters greater than 10m, found in large petroleum refineries. The design of column internals varies widely and is the object of continuing research and development, but its objective is always the same: to provide intimate and effective contact between the rising vapor and the descending liquid. Intimate and effective contact requires a large interfacial area between the vapor and the liquid. Both phases must also have good access to the interface. Thus even if a superficial froth provides a large interfacial area, the contact may be ineffective if most of the bulk liquid is far from the interface. Another requirement is that there be adequate time of contact between the phases to permit mass transfer. This means that there must be sufficient liquid holdup. It is also important that both phases be in a state of sufficent agitation to assure efficient mass transfer within the phases. Finally, it is important to prevent vapor or liquid passing through a stage without adequate interphase contact on that stage (i.e., entrainment).

Meeting all the criteria above requires the establishment of a complex flow structure within a distillation column. While an almost infinite variety of specific designs are used, most column configurations can be divided into two general types: discrete-stage devices and continuous-contact devices. Both are illustrated schematically in the insets of Fig. 1. Discrete-stage devices usually consist of a series of trays with openings to permit the rise of the vapor and the descent of the liquid. A liquid pool of a certain depth resides on each tray, while vapor from the stage below bubbles up through it. In some smaller distillation columns, the liquid may descend by draining through the same openings, but in larger columns (as well as many smaller ones) the reflux descends through larger openings or tubes (called downcomers) located either at the sides or the center of the column cross section. Downcomer locations are offset from one stage to the next so that reflux liquid must flow across the cross-sectional area of the tray before descending to the next tray. Under proper operating conditions, the trays provide for adequate liquid holdup and contact time, while the bubbling action of the rising vapor provides large interfacial area and good intraphase agitation. The tray spacing must be adequate to preclude significant liquid spraying or frothing on one tray from rising to the next.

Continuous-contact devices consist of an open column (undivided by trays) filled with packing elements (rings, saddles, spheres, helices, etc.) or gridworks of various kinds to provide a large interfacial area. The presumption is that descending reflux will wet out the packing or gridwork with a uniformly distributed thin liquid film. The slowed rate of liquid descent provides adequate holdup and contact time with the rising vapor. Although discrete stages are not physically provided in such columns, countercurrent staging nonetheless exists.

Perhaps the most important point of distinction between the discrete-stage and continuous-contact configurations is with respect to the mode of interfacial area formation. In the former case, area is formed as bubbles of vapor are forced through pools of reflux liquid. The amount of area formed bears no direct relationship to the area of the tray or of the holes, but depends more on the bubble size and rate of bubbling. We thus refer to a tray column as an unsupported-area device. It is to be contrasted with the continuous-contact, packed column in which the vapor-liquid interfacial area does depend directly on the amount of solid surface area made available. A packed column is thus referred to as a supported-area device.

For either type of column construction, the internal flow scheme is highly complex, and vapor and liquid flow rates must be maintained within careful ranges for satisfactory operation. If the flow rate is so great that the countercurrent flow of the opposite phase is impeded, the column is said to be flooded. On the other hand, if the flow rates are too low, phase distribution and contact will usually be poor, and in any event, the column is operated at below its design capacity. Flow rates are generally adjusted to a certain percentage (50 to 80%) of the corresponding flooding values for optimal operation.

III. THE EFFECT OF SURFACE TENSION ON FLOW STRUCTURE

Because of the complexity of the flow structure existing in distillation equipment, it is useful to subdivide it into simplified flow elements which might be amenable to more quantitative discussion or to analysis. Such a breakdown makes it possible to show how surface tension or capillary effects influence the flow structure. We first consider how liquid surface tension level effects the flow structure, ignoring for the moment the existence of surface tension gradients which necessarily exist in the multicomponent interfaces present in distillation. Thus in this section, attention is focused on the behavior of pure liquids or liquid mixtures which do not produce significant surface tension gradients in order to separate out the influ-

ence of capillary effects in the absence of tension gradients. These will be discussed in detail in succeeding sections.

In tray columns (unsupported-area devices) the primary processes are the formation, detachment, and rise of vapor bubble through liquid pools, as pictured in Fig. 2. When the bubbles reach the surface, they may either burst immediately into a spray of droplets, or they may exist briefly in a froth layer atop the liquid pool. When the bubbles burst, small jets are formed that pinch off into droplets under the influence of surface tension by the mechanism described originally by Rayleigh [6]. Rayleigh theory predicts that the jet length varies inversely with the square root of surface tension, but the drop size is independent of it. The bubble size and frequency in a given case are found to depend in complicated ways on the hole size, liquid depth, vapor velocity and liquid density, viscosity, and surface tension [7]. The effect of surface tension alone is difficult to separate out, but in general a decrease in surface tension level leads to larger bubbles, other factors remaining the same. Fane and Sawistowski [8] claim that the magnitude of the surface tension plays an important role in determining the efficiency of tray columns operating in the spraying regime. They produced data showing tray efficiency inversely proportional to surface tension, explaining some of the low efficiencies obtained in vacuum distillation (lower temperature, hence higher surface tension). Andrew [9], on the other hand, investigated the froth height developed on a small glass sieve plate by a variety of liquids and found it to be independent of surface tension. The existence of a froth or foam on

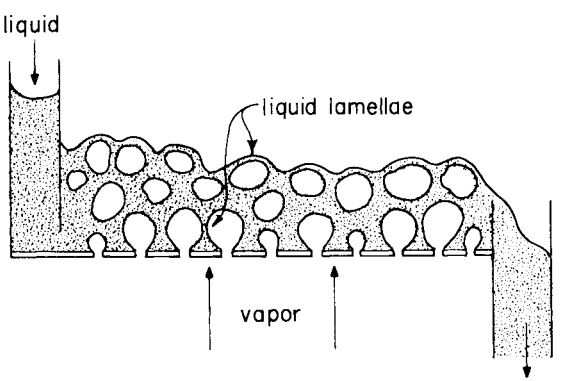

FIG. 2 Schematic of vapor and liquid flows on a tray. Liquid downcomers are shown at left and right. Liquid lamellae between rising bubbles and between bubbles and vapor above the tray are indicated.

top of the liquid on a tray cannot be supported by a pure liquid, but is generally associated with multicomponent systems in which surface tension gradients exist [10], as explained later, and in particular with the presence of surface-active contamination. The existence of any frothing at all with "pure" liquids, as reported for example by Andrew, is probably attributable to such contamination. In summary, attempts to correlate the flow structure on or the distillation efficiency of tray columns with the surface tension of the distillation mixture have not produced convincing generalizations.

In packed columns (supported-area devices) the flow element is that of a thin liquid film flowing downward over a solid surface. The film may be coherent and of essentially uniform thickness, or it may be punctuated with dry patches of varying size. In the extreme, the dry patches may occupy most of the solid surface area, with the liquid flowing downward in rivulets or drops. If the liquid film is coherent, the surface tension level plays no role in its flow properties (thickness, velocity profile), but it does play an important role in determining whether dry patches will develop and persist (i.e., whether or not they will be spontaneously rehealed). This may be understood in the following way. A liquid film is always subject to disturbances which will lead to the existence of local thin spots. Also, the irregularities introduced by the sharp edges of the packing elements always produce local thin spots in the film. A hydrodynamic stability analysis by Jain and Ruckenstein [11] examines the fate of such disturbances. The results show that whenever the thickness of the film is of the order of a few hundred angstroms or less, it will spontaneously thin itself and rupture, leaving a dry patch. This process can occur very rapidly. Depending on the nature of the liquid-vapor-solid interline, the dry patch may reheal itself so quickly that its occurrence is scarcely noticeable, or it may persist and even grow in size. The factor that dictates the existence of dry patches is thus the ability of the film to reheal itself.

For pure-liquid isothermal films, dry patch persistence is determined by a balance between surface tension forces and those of fluid pressure. Performing such a force balance, Hartley and Murgatroyd [12] determined that the minimum wetting rate required to reheal a dry patch on a vertical surface is given by

$$\frac{\dot{m}}{W} = K\left(\frac{\mu\rho}{g}\right)^{1/5} [\sigma\,(1 - \cos\,\theta)]^{3/5} \qquad (1)$$

where $\dot{m}/W$ is the mass flow rate of the liquid per unit width; g the gravitational constant; μ, ρ, and σ the viscosity, density, and surface tension of the liquid, respectively; and θ the contact angle.

K is a constant that depends on the system of units chosen. Comparison of Eq. (1) with experimental data bears out the trends of its predictions.

The contact angle, θ, is a quantitative measure of the physical interaction between a liquid and a solid. As indicated in Fig. 3, it is the angle made by the liquid against the solid, measured in the liquid. If $\theta = 0°$, the liquid "wets out" the solid; if $0 < \theta < 90°$, the solid is "wet" by the liquid; and if $\theta > 90°$, the solid is said not to be wet by the liquid. Under equilibrium conditions, the contact angle may be related to the surface tension of the liquid and the surface energies of the solid-vapor and solid-liquid interfaces by Young's equation [13]:

$$\cos \theta = \frac{\sigma_{SV} - \sigma_{SL}}{\sigma_{LV}} \tag{2}$$

where $\sigma_{SV} = (\partial F/\partial A_{SV})_{T,V}$ and $\sigma_{SL} = (\partial F/\partial A_{SL})_{T,V}$, in which F is the Helmholz free energy of the system, A_{ij} is the area of the appropriate interface, and the derivatives are taken under conditions of constant temperature and volume. It is also presumed in defining these "interfacial tensions," σ_{SV} and σ_{SL}, that adsorption equilibrium exists. $\sigma_{LV} \equiv \sigma$ = the surface tension of the liquid.

Equation (1) implies that dry patch persistence is extraordinarily sensitive to the contact angle. The critical wetting rate at $\theta = 20°$, for example, is more than twice the rate at $\theta = 10°$ and more than five times the rate at $\theta = 5°$, at the same surface tension. It should be noted that the contact angle generally exhibits a significant difference in value depending on whether the liquid is advancing or receding over the solid surface, the advancing angle being larger than the receding angle. Such hysteresis is well understood in terms of solid surface roughness and chemical (energetic) heterogeneity

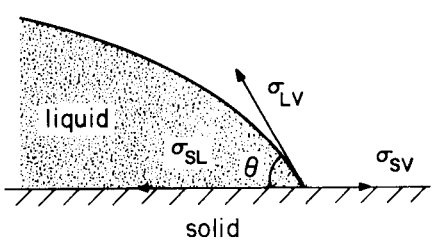

FIG. 3 The contact angle θ, of a liquid against a solid.

[14], but raises some ambiguities in the application of Young's equation. It is clear, however, that it is the advancing contact angle that is relevant to the question of rewetting a dry patch. It is interesting to note in retrospect that while the value of this contact angle plays no role in determining the initial instability of the film to dry patch formation, it is the dominant factor in their removal, as shown in the experiments of Silvi and Dussan [15].

The role of liquid surface tension level is seen by substitution Eq. (2) into Eq. (1) to obtain

$$\frac{\dot{m}}{W} = -K \left(\frac{\mu\rho}{g}\right)^{1/5} [\sigma_{SV} - (\sigma_{SL} + \sigma_{LV})]^{3/5} \qquad (3)$$

where the quantity in brackets is the "spreading coefficient" of the liquid on the solid. It is negative for liquids that do not wet out the solid. For liquids that do spontaneously wet out a solid, no flow need be imposed to assure the destruction of the dry patch. Other factors remaining unchanged, a reduction in the surface tension will lead to more even wetting of the packing (i.e., to fewer and smaller dry patches). On the other hand, solid surfaces of high energy (high σ_{SV}), such as clean metals and most ceramic materials, should be more easily wet than lower-energy materials such as the various plastics.

The consequences of liquid film differences (i.e., whether the liquid film is coherent or broken up into dry patches and rivulets) in a packed distillation column are multifold. Of greatest importance is the reduction in available interfacial area accompanying the breakup of a film into dry patches and rivulets. This can produce a marked drop in the mass transfer efficiency of the unit. Coughlin [16] investigated the mass transfer efficiency and other characteristics of a 15mm x 76mm column packed with 10-mm ceramic Raschig rings (which were wet out by the liquid) compared to those of the same column packed with rings of Saran polymer and pothyethylene, both of which were poorly wet. The operation studied was the absorption of oxygen from air into an aqueous solution of sodium sulfite. The measured contact angles of the liquid test solution against the Saran and polyethylene were 66° and 78°, respectively, as compared to 0° for the ceramic material. The wetting differences between the polymeric materials and the ceramic packing produced little difference in the pressure drop or the operating holdup, but produced a marked decrease in the drainage time for the operating holdup and increased the tendency of the column to exhibit loading. Most important, the poorer wetting of the polymeric packing produced a 20% reduction in overall mass transfer efficiency. One would expect interfacial area reductions caused by film breakup to have the great-

est effect on efficiency on those systems for which the mass transfer is vapor-phase controlled (i.e., for which the major resistance to mass transfer lies in the vapor phase). This situation is characteristic of most distillation operations. When the mass transfer resistance of the liquid film dominates, the process of film breakup may produce sufficient agitation of the liquid to increase the mass transfer coefficient in that phase, partially offsetting the effect of reduced area. Coughlin's results are consistent with those of Sherwood and Holloway [17], who compared the efficiencies of gas stripping in columns packed with paraffin-coated packing elements with those using clean packing.

King and Walmsley [18] compared the efficiency of a stainless steel Stedman packing for the distillation of a water-deuterium mixture against that of an organic test mixture and found good wetting and high efficiency for the latter but not the former. The surface tension of the organic liquid was sufficiently low to produce good wetting. The performance of the packing was significantly improved by cleaning it with potasium permanganate solution. It is well known that unclean metal surfaces generally bear a thin layer of organic contaminant which is poorly wet by most liquids, in contrast to clean metal surfaces, which are wet out by most liquids.

One apparent resolution to the problem of poor wetting in a packed column is to increase the liquid rate, as suggested by the results of Hartley and Murgatroyd [12]. Generally, however, it cannot be raised sufficiently without exceeding the flooding limit. It is thus important to choose a packing material that is wet out by the liquid to be distilled. Reducing the surface tension level and thereby improving wetting through the use of surfactants (wetting agents) may be useful, but the consequences of their presence are more complex than a simple surface tension reduction (as explained later) and may entail undesirable side effects, such as premature flooding of the column.

IV. SURFACE TENSION GRADIENTS: THE RESULTS OF ZUIDERWEG AND HARMENS

In a landmark paper published in 1958, Zuiderweg and Harmens [19] demonstrated that in distillation, it is more the development of surface tension gradients than the surface tension level that plays a dominant role in determining the flow configuration and efficiency in both unsupported-area and supported-area equipment. They examined a wide variety of binary distillations in bench-scale equipment of both types. It is instructive to look at a sample of their results: a comparison of a distillation of a mixture of *n*-heptane and toluene with a distillation of a mixture of benzene and *n*-heptane. When the *n*-heptane/

toluene mixture, at an average *n*-heptane concentration of 40 mol %, was distilled in a Oldershaw sieve tray column at vapor velocities between 0.13 and 0.29 m/s, the froth height was observed to be 60mm, and the tray efficiency was 97 to 100%. In contrast, when the benzene/*n*-heptane mixture, at an average benzene concentration of 40 mol % was distilled in the same column at vapor velocities between 0.14 and 0.62 m/s, the froth height varied between 10 and 20mm, and the tray efficiency was 52 to 55%. What froth was observed in the latter system seemed to consist of larger bubbles which tended to burst into a spray of droplets. This type of spraying was not evident in the more frothy, efficient systems. The observation that the efficiency of a tray column operating with a "foaming" system was often double that of a column operating with a spraying system is consistent with results reported by several earlier investigators [20–22].

A similar comparison was made when the two mixtures, both with an average concentration of the more volatile component equal to 65 mol %, were distilled in a column packed with Fenske helices at a vapor velocity of 0.06 m/s. The height of packing equivalent to a theoretical plate (HETP), a measure of the mass transfer efficiency in the column (low HETP = high efficiency), was 15mm for the *n*-heptane/toluene system but 30mm for the benzene/*n*-heptane system. It was difficult to see a large difference in the flow behavior between the two cases in the packed column, but when a similar comparison was made in a wetted-wall column, it was noted that in the *n*-heptane/toluene system (system A), the condensate film was uniform and stable, whereas in the benzene/*n*-heptane system (system B), the film broke up into distinct rivulets. The latter type of behavior in the packed column would lead to reduced interfacial area and reduced mass transfer efficiency, as was in fact observed.

Differences similar to those detailed above were observed for several other systems, including one that has an azeotrope near the middle of the composition range (viz., ethanol and 2,2,4-trimethylpentane). At ethanol concentrations below the azeotrope (53 mol %), the system behaved like that of system B above, while at ethanol concentrations above 53 mol %, it behaved like system A.

Zuiderweg and Harmens explained these differences by examining the properties of the two different systems, as shown in Table 1. In system A, the more volatile component has the lower surface tension, while in system B this is reversed. The high-efficiency characteristics of systems of type A compared to the low efficiency of those of type B were observed for all the systems studied, including the azeotrope. These two types of systems were designated as surface tension positive (σ^+) and surface tension negative (σ^-), respectively, as shown in Fig. 4. For σ^+ systems, surface tension in-

TABLE 1 Comparison of Component Properties

	System A	
Component	*n*-Heptane	Toluene
Boiling point	98.4°C	110.6°C
Surface tension	20.2 mN/m	28.5 mN/m
	System B	
Component	Benzene	*n*-Heptane
Boiling point	80.1°C	98.4°C
Surface tension	28.8 mN/m	20.3 mN/m

creases as one moves downward in the column, while for σ^- systems, it decreases moving downward. Systems for which the component surface tensions are essentially equal (within 1 or 2 mN/m of each other) were designated surface tension neutral. Neutral systems behaved essentially as σ^- in tray columns and σ^+ in packed towers. The explanation of Zuiderweg and Harmens for the difference in behavior between the two types of systems relies on the development of surface tension gradients as described below for both unsupported-area and supported-area equipment. Other investigators have since added to the data base of Zuiderweg and Harmens. For example, Medina et al. [23] measure foaming and efficiency of several addition-

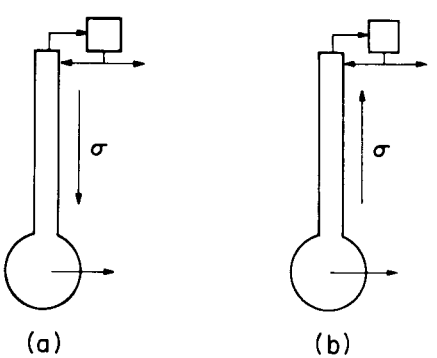

FIG. 4 Schematic of distillation column showing the variation of surface tension in (a) a σ^+ system and (b) a σ^- system.

al binary systems and one ternary system in a sieve plate column and found the same trends as those reported by Zuiderweg and Harmens. With respect to the ternary system, two distinct zones of composition were observed, in one of which the system was σ^+ and the other in which it was σ^-, as determined by whether surface tension was increasing or decreasing, respectively, moving down the column. Moens [24,25], on the other hand, looked at additional binary systems in packed tower distillation columns and also found results consistent with Zuiderweg and Harmens.

A. Unsupported-Area Equipment

Consider the thin lamella of liquid between adjacent vapor bubbles on a tray or the lamella that encloses a vapor bubble as it emerges from the liquid pool on a tray, as shown schematically in Fig. 2. The enlarged view of a section of such a liquid film is shown in Fig. 5, which emphasizes that such films will always develop nonuniformities in thickness. Zuiderweg and Harmens argued that the thinner sections of such films would be closer to being in equilibrium with the vapor phase than would the thicker portions, and therefore relatively leaner in the more volatile component. In σ^+ systems, this would result in the thinner areas of the lamella having higher surface tension than the adjacent thicker areas, so that the surface tension gradient developed would tend to restore uniformity in film thickness, as shown. In σ^- systems, the surface tension gradients would develop in just the opposite sense, so that rapid film drainage, bubble coalescence, and bursting would be favored. Liquid films in the absence of any surface tension gradients will very rapidly thin down and rupture. Whenever a film is formed, as shown in Fig. 6, a capillary pressure driving force is set up to cause thinning in the following way. The pressure difference, ΔP, which exists across a fluid interface, is given by the Young-Laplace equation [13],

$$\Delta P = \sigma\kappa \tag{4}$$

where κ is the curvature of the interface. The pressure is always greater on the concave side of the interface. Thus at point A, where the interface is flat ($\kappa = 0$), $\Delta P = P_{vap} - P_{liqA} = 0$, but at point B, $P_{liqB} < P_{vap} = P_{liqA}$. Thus since $(P_{liqA} - P_{liqB}) > 0$, there will be a spontaneous flow toward the edge of the film, resisted only by negligible fluid inertia. When the lamella thickness reaches a value of a few hundred angstroms, it becomes unstable with respect to disturbances that lead to its rupture, as predicted by the stability analysis of Vrij et al. [26] and confirmed by the experiments of Sheludko [27]. The process of thinning and rupture is virtually instantaneous under the circumstances described. If countering surface